https://doi.org/10.5194/gmd-2020-68
Preprint. Discussion started: 28 April 2020


Geoscientific Model Development Discussions

# Sensitivity of aerosol optical properties to the aerosol size distribution over central Europe and the Mediterranean Basin

Laura Palacios-Peña[1], Jerome D. Fast[2], Enrique Pravia-Sarabia[1], and Pedro Jiménez-Guerrero[1]

[1]Physics of the Earth, Regional Campus of International Excellence "Campus Mare Nostrum", University of Murcia, Spain.
[2]Pacific Northwest National Laboratory, Richland, WA, USA

**Correspondence:** Pedro Jiménez-Guerreo (pedro.jimenezguerrero@um.es)

**Abstract.** Aerosol size distribution is, among others, a key property of atmospheric aerosols when trying to establish the uncertainties related to aerosol-radiation (ARI) and aerosol-clouds (ACI) interactions. These interactions ultimately depend on the size distribution through optical properties as aerosol optical depth (AOD) or cloud microphysical properties. Hence, the main objective of this work is to study the impact of the representation of aerosol size distribution on aerosol optical properties over Central Europe, and particularly over the Mediterranean Basin during a summertime aerosol episode. To fulfill this objective, a sensitivity test has been carried out using the WRF-Chem on-line model. The test consisted on modifying the parameters which define a log-normal size distribution (the geometric diameter, from now on DG, and the standard deviation, SG) by 10, 20 and 50 %. Results reveal that the reduction in the SG of the accumulation mode leads to the largest impacts in the AOD representation due to a transfer of particles from the accumulation mode to the coarse mode. A reduction in the DG of the accumulation mode has also an influence on AOD representation since particles in this mode are assumed to be smaller. In addition, an increase in the DG of the coarse mode produces a redistribution through the total size distribution by relocating particles from the finer modes to the coarse.

## 1 Introduction

Aerosol size distribution is, among others, a key property of atmospheric aerosols which largely determines their interaction with radiation and clouds. This is because aerosol optical properties, such as the scattering phase function, single scattering albedo, or the aerosol optical depth (AOD), strongly depend on the aerosol size distribution (Eck et al., 1999; Haywood and Boucher, 2000; Romakkaniemi et al., 2012; Obiso et al., 2017; Obiso and Jorba, 2018). Thus, the latter holds a strong influence on aerosol-radiation interactions (ARI) and their associated radiative forcing (Boucher and Anderson, 1995; Boucher et al., 1998; Myhre and Stordal, 2001).

On the other hand, atmospheric aerosols have an influence on climate forcing through aerosol-clouds interactions (ACI). These interactions produce an impact on clouds and precipitation which depends on the number concentration of particles,

https://doi.org/10.5194/gmd-2020-68
Preprint. Discussion started: 28 April 2020


Geoscientific Model Development Discussions

which can act as cloud condensation nuclei (CCN) and ice nuclei (IN). Ultimately, these condensation nuclei depend on the aerosol size distribution and composition (Andreae and Rosenfeld, 2008; Romakkaniemi et al., 2012).

The aerosol size distribution represents the number (N); mass (M); or volume (V) of particles as a function of radius (r; Seinfeld and Pandis, 2006). Commonly, the aerosol size distribution is represented as a function of the logarithm of radius. Thus, the total number; mass; or volume of aerosol particles is the integral of the radius over the size distribution function (Buseck and Schwartz, 2003).

In this sense, the representation of aerosol processes in meteorological or climate models presents a high uncertainty (Boucher et al., 2013). Particularly, modeling aerosol size distribution introduces a noticeable uncertainty in chemistry transport models (Tegen and Lacis, 1996; Claquin et al., 1998). When aerosol size distribution is modeled, three different approaches are commonly used (Boucher, 2015): (1) First, a bulk approach in which only the aerosol mass concentration is computed. A constant size distribution is assumed and there is not a representation of a mixing state which results in a simple and computationally cheap approach . (2) A more complex approach consists in the use of multiple superposed modes which typically are represented by a log-normal distribution described by a fixed mean and variance. The accuracy of this approach lies in the correct choice of these two parameters. (3) Last, the most computationally expensive approach is the sectional representation, which consists in discretizing the aerosol size distribution into $n$ classes or bins of radius where the concentration of aerosols in each bin follows the conservation equation and then the number; mass; or volume in each bin is predicted.

When a size distribution is considered, a log-normal approach is typically employed in chemistry transport models because this distribution fits observed aerosol size distribution reasonably well and its mathematical form is convenient for dealing with the moment distribution. In a log-normal distribution, all of the moment distributions are log-normal and present the same geometric mean radius and geometric standard deviation, parameters which determine the log-normal distribution (Hinds, 2012). Thus, aerosol size distribution can be described by a log-normal distribution in number (first moment), mass (third moment) and volume (fourth moment) using the same parameters which determine the log-normal distribution.

In addition to the complexity of characterizing adequately the representation of aerosols, the complexity of the target area where the model is applied (e.g. orography, emissions or chemical transport) hampers the correct representation of atmospheric aerosols. Particularly, Europe (and especifically the Mediterranean Basin) is one of the most climatically sensitive regions in the world to aerosol forcing (Giorgi, 2006). Not only anthropogenic aerosol but also sea salt; desert dust and biomass burning, in particular from summer wildfires are presented over the Mediterranean Basin. Particularly in summer, when the aerosol forcing is the largest (e.g. Charlson et al., 1992), the effect of ARI and ACI over this area is crucial (Papadimas et al., 2012) even more than over central Europe (Andreae et al., 2002). This is because of the complex terrain and the geographical location in addition to the processes which these aerosols particles suffer(e.g. intense formation, accumulation and recirculation; Millán et al., 1997; Pérez et al., 2004; Querol et al., 2009)

Due to the important effects of size distribution and because previous works have pointed out to the misrepresentation in size distribution by models (e.g. Palacios-Peña et al. (2017), Palacios-Peña et al. (2018) or Palacios-Peña et al. (2019a)), this contribution analyzes the sensitivity of aerosol optical properties to the representation of aerosol size distribution over Central Europe, and particularly over the Mediterranean Basin. For that purpose, a modeling perspective has been used for a typical

https://doi.org/10.5194/gmd-2020-68
Preprint. Discussion started: 28 April 2020


Geoscientific Model Development Discussions
Open Access
EGU

case study during summertime with the main objective of estimating the sensitivity of AOD to the log-normal distribution parameters (geometric diameter and standard deviation) that characterize the size distribution. This parameters will finally influence the representation of ARI and ACI in meteorological/climate models. Section 2 describes the methodology used to carry out this work and the model setup. Section 3 shows the results found; and Section 4 discusses and summarizes the results.

## 2 Methodology

The case study covers a period between 4 and 9 of July, 2015. The meteorological situation presents a high stability with a high aerosol load, fire emissions in the target area, and a strong dust outbreak over the studied Mediterranean Basin. The choice of this episode reveals the crucial role of aerosols from different sources over the Mediterranean Basin, whose forcing is even stronger in summertime.

A sensitivity test has been carried out to analyze the response of AOD to size distribution. The test consisted in the modification of the geometric diameter (DG) and the standard deviation (SG) of the log-normal function representing the aerosol size distribution. Each parameter has been modified by $\pm$10, 20 and 50 % of its initial value in each of the three modes represented (Aitken, accumulation and coarse).

In order to elucidate how important the changes of AOD are in each experiment and to avoid the analysis of random changes, a Kolmogorov-Smirnov test (Stephens, 1974) has been applied. This is a non-parametric test which can be used to compare two samples by their probability distribution (Stephens, 1974). In this case, all the experiments are compared with the base case to shed light on which changes are more important. The cases with a larger importance will be considered as reference cases to disentangle the causes of the changes in AOD provoked by the modification of the size distribution parameters.

### 2.1 Model setup

The Weather Research Forecast model coupled with Chemistry (Grell et al., 2005, WRF-Chem;) version 3.9.1.1 was used in this work. This fully coupled on-line model represents ARI and ACI by allowing the treatment of meteorology along to gases and aerosols emissions, transport, mixing, and chemical transformation simultaneously.

The case study selected here trusts on an extended episode evaluated in Palacios-Peña et al. (2019b). The model setup for all the experiments is the same as for that work. However, a brief summary of the configuration is included here. The model physics configuration is constituted by: the Morrison microphysics (Morrison et al., 2009); the Rapid Radiative Transfer Model short and long wave radiation schemes (Iacono et al., 2008, RRTM;); the Yonsei University scheme planetary boundary layer (PBL) scheme(Hong et al., 2006, YSU;); the Grell-Freitas ensemble cumulus scheme (Grell and Freitas, 2014) and the Noah soil option (Tewari et al., 2004). Meteorological initial and boundary conditions were provided by the ERA-Interim reanalysis (Dee et al., 2011). The WRF-Chem option for idealized gases and aerosol profile has been chosen as chemical boundary conditions. The chemical configuration include: the Regional Atmospheric Chemistry Mechanism-Kinetic Pre-Processor gas-phase scheme (Stockwell et al., 1997; Geiger et al., 2003, RACM-KPP); the Global Ozone Chemistry Aerosol Radiation

https://doi.org/10.5194/gmd-2020-68
Preprint. Discussion started: 28 April 2020


Geoscientific Model Development Discussions
Open Access
EGU

and Transport model aerosol scheme (Ginoux et al., 2001; Chin et al., 2002, GOCART;); Fast-J (Wild et al., 2000) for the photolysis; dry deposition is estimated by Wesely (1989) and wet deposition is also calculated with grid-scale wet deposition.

Anthropogenic emissions were provided by the Emissions Database for Global Research-Task Force on Hemispheric Transport of Air Pollution (EDGAR-HTAP) project (http://edgar.jrc.ec.europa.eu/htap.php; Janssens-Maenhout et al., 2012). Biomass burning emission data have been estimated from the Integrated monitoring and modelling system for wild-land fires (IS4FIRES; Sofiev et al., 2009; Soares et al., 2015). Both have been adapted to chemical species in WRF-Chem following Andreae and Merlet (2001) and Wiedinmyer et al. (2011); and plume rise calculation was on-line estimated by WRF-Chem. Biogenic emissions are on-line coupled with WRF-Chem by using the Model of Emissions of Gases and Aerosol from Nature (MEGAN; Guenther et al., 2006). Finally, dust (Ginoux et al., 2001) and sea salt GOCART (Chin et al., 2002) emissions were on-line estimated by WRF-Chem.

The target domain covers central Europe and the Mediterranean Basin with a resolution of $\sim 0.15\,^{\circ}$ ($\sim$16.7 km, Figure 1), but this domain was run using nested domains in order to capture the total desert dust contribution from the Sahara Desert. For that purpose, a parent domain covering the main areas of desert dust emissions (located around 15 °N) was used. The other domains were built by one-way nesting with a nesting ratio of 1:3 with respect to its larger domain. Thus, the parent domain has a spatial resolution of $1.32\,^{\circ}$ (150 km) and the second of $0.44\,^{\circ} \sim 50$ km. Vertical resolution presents 48 uneven layers establishing the top of the atmosphere at 50 hPa and the highest resolution at the bottom.

As mentioned above, the aerosol scheme used is GOCART (Ginoux et al., 2001; Chin et al., 2002), which includes a bulk approach. This is a simple and cheap computational approach. The selection of this scheme is conditioned by the fact that WRF-Chem version 3.9.1.1 only allows the simulation of desert dust and sea salt with this GOCART scheme.

The aerosol optical properties module in WRF-Chem calculates optical properties from species estimated by the GOCART scheme. These properties depend on size and number distribution, composition and aerosol water. For a bulk approach as GOCART, bulk mass and number is converted into an assumed log-normal modal distribution, then dividing the mass into sections or bins ("$i$"). The parameters which define this log-normal distribution are the modified variables for the sensitivity test. Then the aerosol optical calculation follows the process described in Barnard et al. (2010). For each bin and each chemical specie ("$j$"), mass is converted to volume. Summing over all the species volume and assuming spherical particles, a diameter ($D$) is assigned to each bin. Therefore, the aerosol size distribution is defined by the number and the associated diameter for each bin. Aerosol water content depends on relative humidity (RH) and the hygroscopicity factor of each species in the aerosol composition. Refractive indices are averaged, by Maxwell-Garnett approximation (Bohren and Huffman, 2007), among the compositions for each section in which mass has been divided. All particles within a size range are assumed to have the same composition, although their relative fraction can differ among size ranges. Finally, an approximate version of the Mie solution (Ackerman and Toon, 1981) is used to estimated the absorption efficiency ($Q_{a,i}$), the scattering efficiency ($Q_{s,i}$) and the asymmetry parameter ($g_i$). Optical properties are computed by summing over the size distribution. The equation bellow shows the example for the estimation of the scattering coefficient ($\sigma_s$):

https://doi.org/10.5194/gmd-2020-68
Preprint. Discussion started: 28 April 2020


Geoscientific Model Development Discussions

$$\sigma_s = \sum_{i=1}^{8bins} N_i Q_{s,i} \pi (\frac{D_i}{2})^2 \quad (1)$$

## 3 Results

First the effects of the sensitivity test on AOD representation are investigated. Afterwards, the magnitude of these effects is analyzed by using the Kolmogorov-Smirnov test. Once the most relevant cases have been established, the causes of these changes are scrutinized.

### 3.1 Effects on AOD representation

Figure 1 shows AOD at 550 nm simulated by the base case (top row) and the differences between each of the experiments in the sensitivity test and the base case. This Figure only exhibits the results for the modification of 50 %, but the rest of the experiments are shown in the Supplementary Material (Figure 1). The reason to show only the 50 % modification is because the patterns of changes for each experiment are qualitatively similar for the sensitivity tests modifying the parameters by 10, 20 and 50 % but are quantitatively larger on the latter.

Top row in Figure 1 displays the temporal mean of AOD for the target period. As established by Palacios-Peña et al. (2019b), high AOD values over the western part of the Mediterranean Basin and central Europe were caused by a strong desert dust outbreak from the Sahara desert. The eastern part of the Mediterranean AOD also presents high values because the outbreak reached that part at the end of the period. Palacios-Peña et al. (2019b) evaluated the simulation against observations coming from Moderate Resolution Imaging Spectroradiometer (MODIS; and instruments abroad satellite) and the Aerosol Robotic Network (AERONET). The evaluation results demonstrated negligible errors of the model over large areas with temporal mean absolute errors of 0.16 (when assessed against MODIS) and 0.12 (evaluation against AERONET).

Regarding the differences of the sensitivity test, the modeling results are not very sensitive to the modification of the standard deviation for the Aitken mode (L50_SGai and H50_SGai). Identical results are found for the variation of the geometric diameter of the Aitken mode (L50_DGai and H50_DGai). In these experiments there is not a clear pattern in the response of AOD to the modifications implemented; that is, positive and negative low changes (most of them above 0.05) are alternated in the space. Some small areas display higher differences (around and above $>0.1$), in particular, close to the boundaries. When temporal and spatial differences are studied, these differences range between -0.03 and -0.01, which shows that there is not a clear impact of the modification of size distribution for the Aitken mode.

Sensitivity experiments regarding modifications in the accumulation mode lead to higher changes with respect to the Aitken mode; however, sensitivity is still limited. The experiment where the standard deviation of the accumulation mode decreases (L50_SGac) is that with the higher impact on AOD. Over most of the domain the change is $> 0.1$. These changes are negative over central Europe and the Iberian Peninsula (where AOD in the base case is $> 0.3$) and are positive over the eastern Mediterranean Basin. No significant patterns of change are visualized when increasing the the standard deviation of the accumulation

https://doi.org/10.5194/gmd-2020-68
Preprint. Discussion started: 28 April 2020


Geoscientific Model Development Discussions

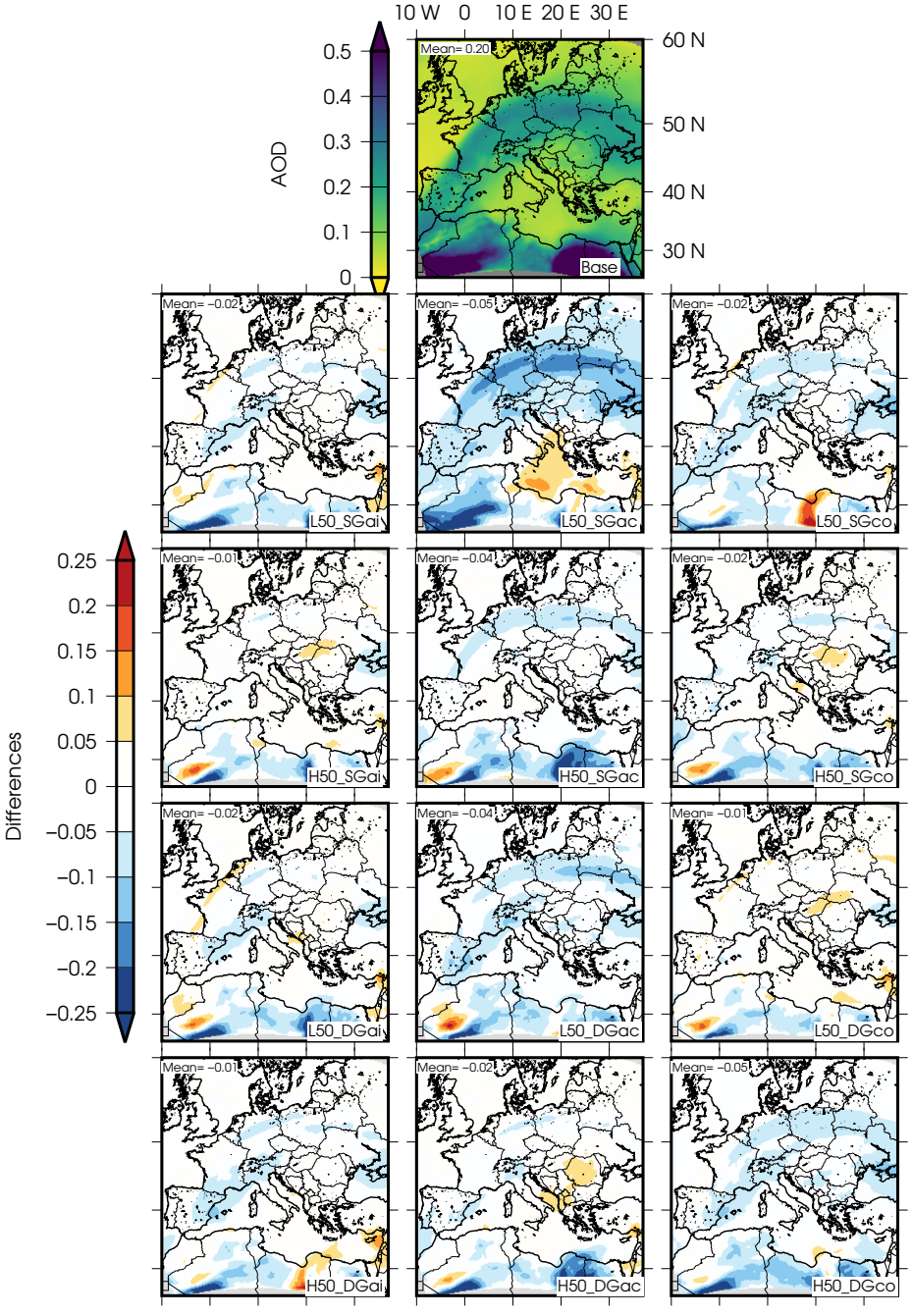


**Figure 1.** AOD at 550nm and differences for simulations of sensitivity test at 50%.

mode (H50_SGac), with changes in AOD under ±0.05. Regarding the experiments that modify the geometric diameter, negative changes with a temporal and spatial mean of -0.04 are found when the DG decreases by 50 %, meaning that, in general, the

https://doi.org/10.5194/gmd-2020-68
Preprint. Discussion started: 28 April 2020


Geoscientific Model Development Discussions

model is considering particles in the accumulation mode smaller than in the base case. On the other hand, when DG increases, positive changes are generally observed, leading to larger particles than in the base case. In spite of this overall signal, positive and negative signals alternate in both simulations.

Finally, when considering changes for the coarse mode, H50_DGco (in which the geometric diameter increases) is the experiment leading to the strongest response. Negative variations are found over a large part of the domain which can reach values up to -0.15 over smaller areas. However, when the DG decreases, the response oscillates between negative and positive values lower than 0.05. Analogously, the modification of the standard deviation for the coarse mode does not show a clear pattern of response to the sensitivity test.

As mentioned previously, for all of the experiments, higher changes (above 0.1) are found close to the south boundary. This could be caused by the fact that the main natural sources of emissions are located in this area.

### 3.2 Significance of AOD changes

This section elucidates the importance of AOD changes, in order to discriminate those experiments more sensitive to changes in the parameters characterizing the size distribution, in order to disentangle the physico-chemical causes behind those changes. For that reason, Figure 2 displays the probability density function (PDF) of the AOD at 550 nm values (in space and time) simulated by the base case (solid black line) and each of the experiments (dashed red line) in the sensitivity test. As in the previous section, this Figure only exhibits the results for the modification of 50 %, but the rest of modifications can be found in the Supplementary Material (Figure 2). The number in each panel represents the statistics obtained from the Kolmogorov-Smirnov test. This test estimates the distance between the cumulative distribution function (represented by D) and how significant this difference is (represented by the p.value).

For all of the experiments (top and bottom; SG and DG; and 10, 20 and 50 %) the distance between the samples is statistically significant (p.value close to 0) because of the high number of samples (cells) in each experiment. As all the spatio-temporal values are taken for statistical purposes, the number of samples is over 1000000. However, the distance varies between each experiment.

L50_SGac is the experiment with the highest distance (0.2277), meaning that this experiment presents the largest difference with respect to the base case. H50_DGco, with a distance of 0.1920, and L50_DGac, with 0.1648, are those with a noticeable difference (distance), but lower than for L50_SGac. H50_SGac, with a distance of 0.0891, also shows differences but not as important as for the former cases. The rest of the sensitivity cases present differences lower than 0.05; that is, differences are small with respect to the base case, although statistically significant.

Similar results are found when the modification of 10 and 20 % are analyzed (Figure 2). These cases exhibit distances lower than for the modification of 50 % but higher than 0.05. The distance is lower as the magnitude of the modification decreases. For example, the L10_SGac distance is 0.0863, the L20_SGac is 0.1814 and the L50_SGac is 0.2270. This behaviour is repeated in the rest of the experiments, but with distances lower than 0.05.

These measured distances can be observed in the PDF shown in the corresponding Figures. The second panel in the first row portraits the PDF for L50_SGac, showing a much higher peak (peak of density higher than 10) than for the base case (peak of

https://doi.org/10.5194/gmd-2020-68
Preprint. Discussion started: 28 April 2020


Geoscientific Model Development Discussions

density lower than 8). Moreover, the upper tail reaches AOD values lower that 3 for the L50_SGac meanwhile the upper tail for the base case reaches AOD values lower than 5. The response for the modification of 20 and 10 % is similar. However, this latter shows larger AOD values in the upper tail and a peak of density lower (around 9).

A similar behaviour is exhibited by the H50_DGco and the L50_DGac cases; but in this latter the upper tail reaches AOD values up to 3. However, the PDF of this experiment does not respond analogously to other quantitative modifications (10

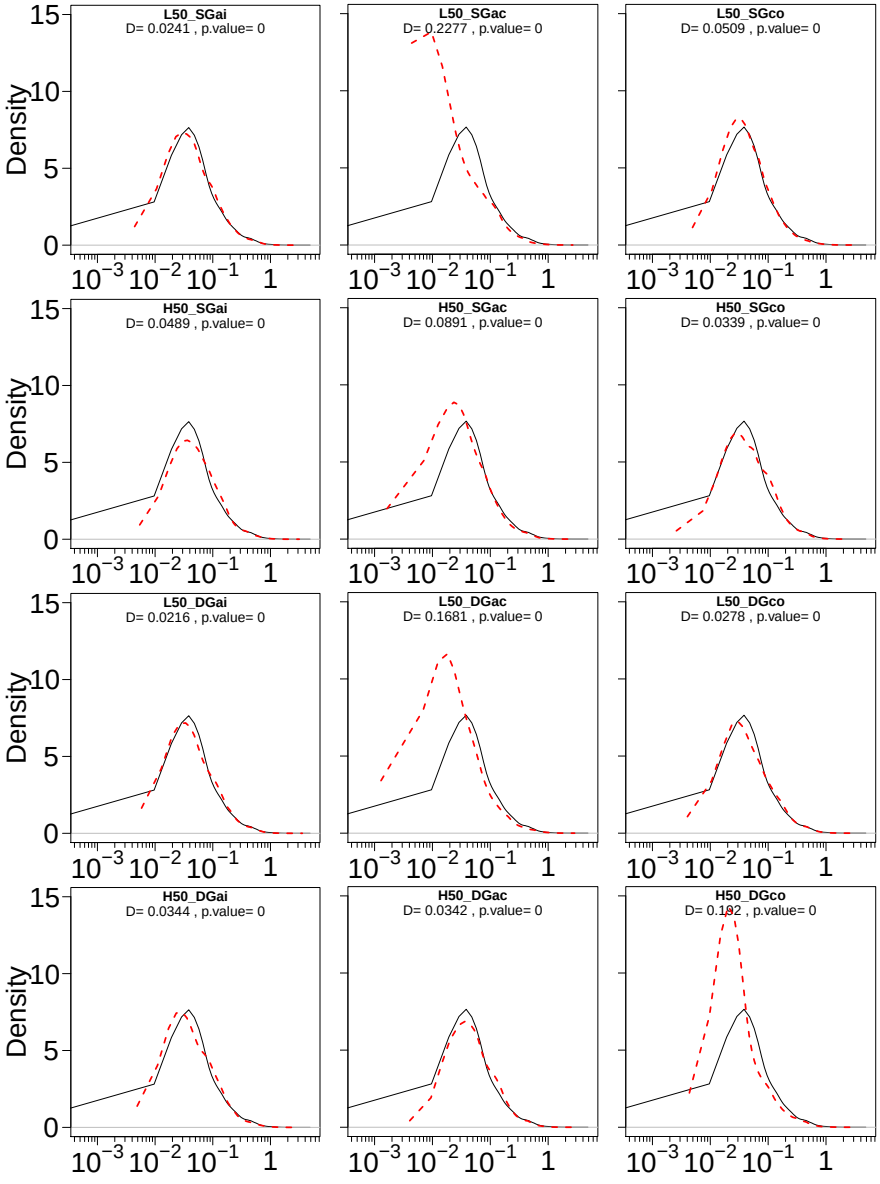


**Figure 2.** PDF of AOD values for sensitivity test simulations at 50 %. Values in Figures represent the results for the Kolmogorov-Smirnov test.

https://doi.org/10.5194/gmd-2020-68
Preprint. Discussion started: 28 April 2020


Geoscientific Model Development Discussions

and 20 %). H50_SGac is noticeable because its peak of density reaches values up to 9 and its upper tail up to 3; however, its distance is much lower (>0.1) than for the previously mentioned cases and decreases as the modification does.

In order to disentangle the causes for the results found in the sensitivity tests, the next section focuses in those cases where the distance in the Kolmogorov-Smirnov test with respect to the base case is $> 0.1$. These are L50_SGac, L50_DGac and H50_DGco. Regarding other modifications, only the L20_SGac (see Figure 2 in Supplementary Material) shows a distance higher than 0.1. The L10_SGac difference is not higher than 0.1 (because of the limited modification of 10 %) but the distance is the highest for this range of modifications, with a value of 0.09.

### 3.3 Disentangling the causes of AOD variations due to size distribution

Figure 3 displays the PM-ratio for the base case at 1000 hPa and the corresponding differences between the experiment at 50 % and the base case. This statistical figure is estimated as the ratio between $PM_{2.5}$ and $PM_{10}$ and represents the predominance of fine ($PM_{2.5}$) or coarse particles ($PM_{10}$) in the air mass. High values of PM-ratio implies a higher proportion of fine particles while low values of the ratio point to the presence of coarse particles.

For the selected cases, Figure 3 shows an inverse behavior of the PM-ratio with respect to the AOD. The experiment decreasing the standard deviation in the representation of the accumulation mode (L50_SGac) presents a reduction up to -0.45 in the PM-ratio (that is, coarse particles become predominant) over the eastern Mediterranean Basin, which matches with the increase modeled for the AOD. This behavior is also reproduced aloft (at 750 hPa, Figure 3) and is consistent with the sensitivities of 20 % and 10 % (Figure 4 in the Supplementary Material). However, for the other experiments the response is weaker.

The experiment decreasing the geometric diameter of the accumulation mode (L50_DGac) does not lead to large differences. This experiment shows a slight increase of the PM-ratio (around 0.05) over the western Mediterranean and central Europe, which points to slight increase in fine particles; and a limited decrease (around -0.05) of the PM-ratio over Italy, Hungary and Romania.

Finally, the experiment increasing the geometric diameter of the coarse mode (H50_DGco) produces a different response. Albeit this experiment presents lower values (up to -0.25) for the PM-ratio over most of the target domain (hence highlighting the increase in the predominance of coarse particles), AOD is also lower in particular over central Europe.

In order to understand these changes, Figure 4 exhibits the total number concentration of particles at 1000 hPa in the Aitken+accumulation (summed) and coarse modes and the relative differences between the different experiments and the base case for the sensitivity tests modifying the parameters by 50 %. Figure 5 is similar to Figure 4 but for total mass concentration. Aloft particles (750 hPa in Figure 5), and sensitivities (20 % in Figure 7 and 12 and 10 % in Figure 9 and 14) as well as non-relative differences (Figures 6, 8, 10, 11, 13 and 15) are available for both total number and mass concentration in the Supplementary Material.

The experiment reducing the standard deviation in the accumulation mode (L50_SGacc) and its lower modifications, L20_SGac and L10_SGac, show a similar response that becomes stronger the larger the modification is. Because of that, only L50_SGacc is analyzed in this contribution as it is representative of changes in SGacc. This experiment leads to a reduction in the total number concentrations (up to -80 % for the Aitken and accumulation modes and -60 % of the base case for the coarse particles)

https://doi.org/10.5194/gmd-2020-68
Preprint. Discussion started: 28 April 2020


Geoscientific Model Development Discussions
Open Access
EGU

and total mass (up to -60 % of the base case for the Aitken and the accumulation modes and -40 % for the coarse mode) over the European continent for all the modes. However, a reduction in the total number concentration is found over the Mediter-

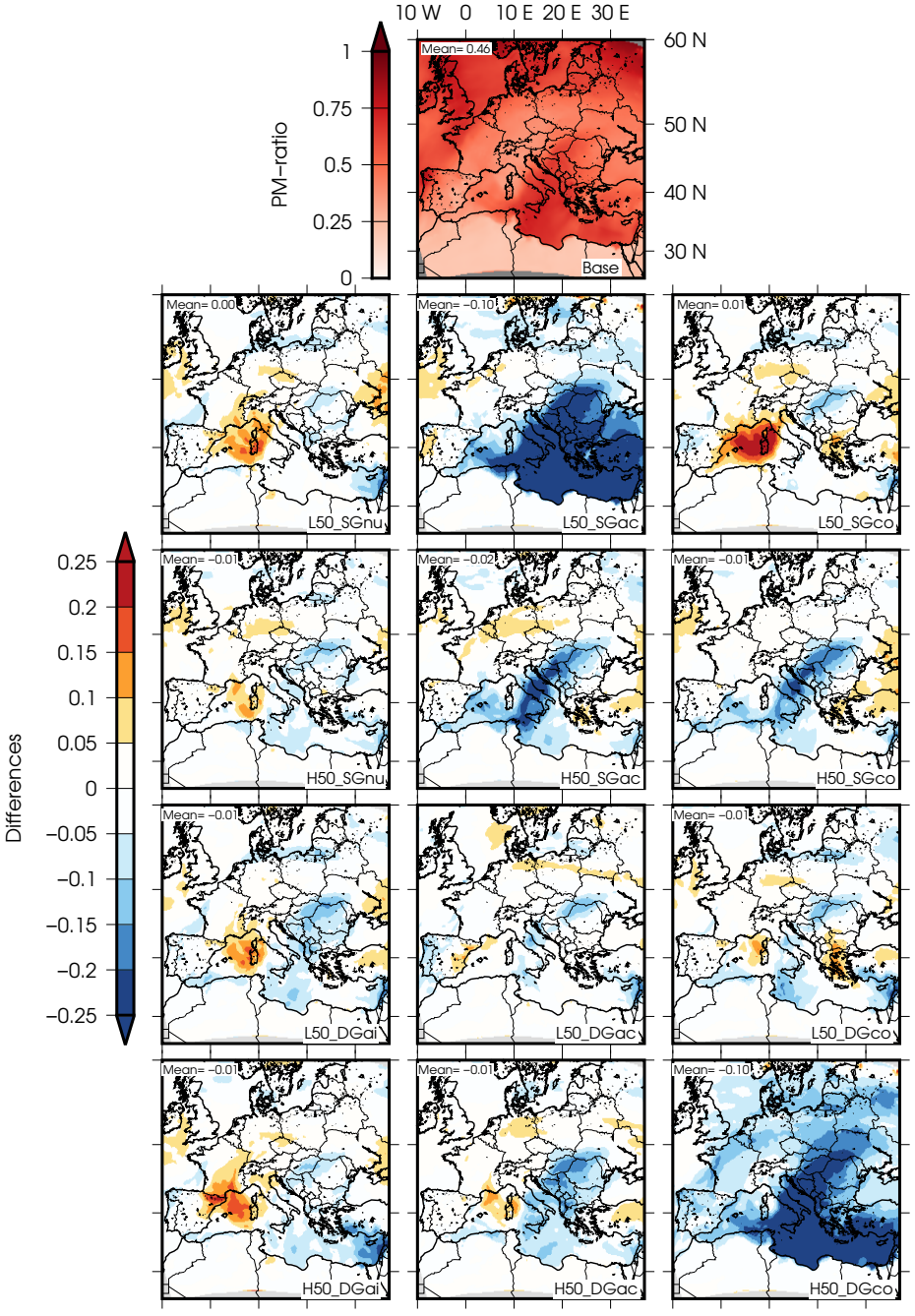


**Figure 3.** PM-ratio at 1000 hPa for the base case and differences for sensitivity test simulations at 50 %.

https://doi.org/10.5194/gmd-2020-68
Preprint. Discussion started: 28 April 2020


Geoscientific Model Development Discussions
Open Access
EGU

ranean and over eastern and western areas for the Aitken and accumulations modes. An increase is depicted over the central and western Mediterranean for the coarse mode (higher than 80 % with respect to the base case). This increase in the total number concentration of the coarse mode could explain the decrease estimated for the PM-ratio and thus the increase in AOD as particles become larger. The reduction in both modes explains the observed decrease in AOD as the number and mass of particles decrease, which does not lead to modifications in PM-ratio because the total number concentration decreases in both modes.

https://doi.org/10.5194/gmd-2020-68
Preprint. Discussion started: 28 April 2020


Geoscientific Model Development
Discussions
Open Access
EGU

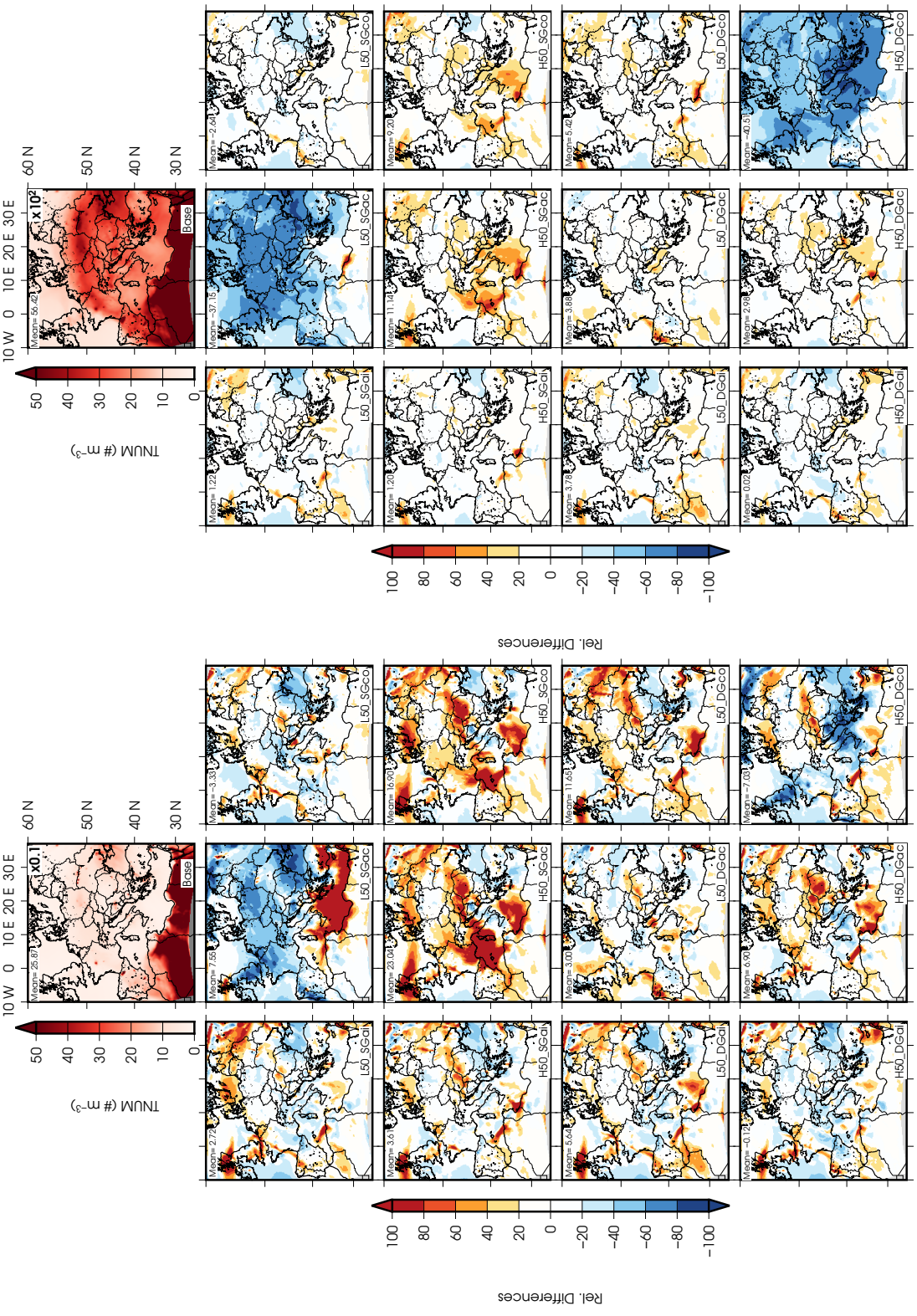


**Figure 4.** Total number concentration of particles at 1000 hPa in the Aitken and accumulation (left) and coarse (right) modes for the base case and relative differences for sensitivity test simulations at 50 %.

https://doi.org/10.5194/gmd-2020-68
Preprint. Discussion started: 28 April 2020


Geoscientific Model Development Discussions

These changes could be attributed to a narrowed distribution in the accumulation mode. This leads to an increase in the number (and mass) of particles in the coarse mode. This increase presents two different scenarios: (1) Over the central Mediterranean Sea, where fine particles dominate, the number of particles in the coarse mode increases and now this type of particles dominates, resulting in an increase of AOD since particles become larger. (2) Over the European continent, where coarse particles come predominantly from the Saharan desert dust outbreak, two aspects have to be highlighted: on one hand, particles are removed from the accumulation mode due to a narrowed size distribution; and on the other hand, an increase in the total number concentration is expected, but this increase favors deposition and finally results in a reduction (smaller than for the accumulation mode) of the total number concentration also in the coarse mode. This preferential removal during atmospheric transport of coarse particles was previously observed by Maring et al. (2003). This reduction does not result in a significantly different PM-ratio because fine particles and coarse particles are removed, but it leads to a decrease in AOD due to a reduction in total mass concentration (see Figure 5).

These changes could also be ascribed to modifications in atmospheric transport patterns caused by the ARI and ACI (taken into account in the simulations), which could alter atmospheric dynamics. However, changes in the sea level pressure (SLP, see Figure 16 in the Supplementary Material), a proxy for changes in the atmospheric transport patterns, are negligible when compared to other works that attribute changes in AOD to modifications in atmospheric dynamics (e.g. Palacios-Peña et al., 2019b).

For the experiment reducing the geometric diameter of the accumulation mode (L50_DGac), the PM-ratio as well as the total number of particles (Figure 4) and mass (Figure 5) concentrations does not show noticeable differences with respect to the base case. Changes over most of the domain in the total number and mass concentrations are below 20 % with respect to the base case. Thus, the reduction observed in the AOD can be attributed to the reduction in the diameter assumed by the log-normal distribution in the accumulation mode. Hence, although mass and number concentrations are similar, the model is assuming that particles in the accumulation mode are smaller than in the base case and this results in a reduction of AOD.

Finally, the sensitivity experiment increasing the geometric diameter of the coarse mode (H50_DGco) leads to a general reduction of AOD, which in this case is associated to a reduction in PM-ratio. When the total number concentration is evaluated, the sum of Aitken and accumulation mode exhibits a reduction up to -60 % with respect to the base case over most of the domain. However, for the coarse mode the total number concentration remains roughly constant. Thus, the reduction in AOD comes from the decrease in the total number concentration in the Aitken and accumulation modes. It should be highlighted that while in the coarse mode the total number concentration remains roughly constant, the total mass concentration increases (>80 % with respect to the base case over located areas) likely because particles with a higher diameter are considered. Similar results were found by Porter and Clarke (1997), whose data demonstrated that both the accumulation and coarse mode aerosol gradually shifted to larger diameters as the aerosol mass increased. Regarding the mass and number reduction in the Aitken and accumulation modes, this comes from a redistribution through the total size distribution caused by the increase in the coarse diameter, which produces a relocation of number and mass particles from the finer modes to the coarser.

https://doi.org/10.5194/gmd-2020-68
Preprint. Discussion started: 28 April 2020


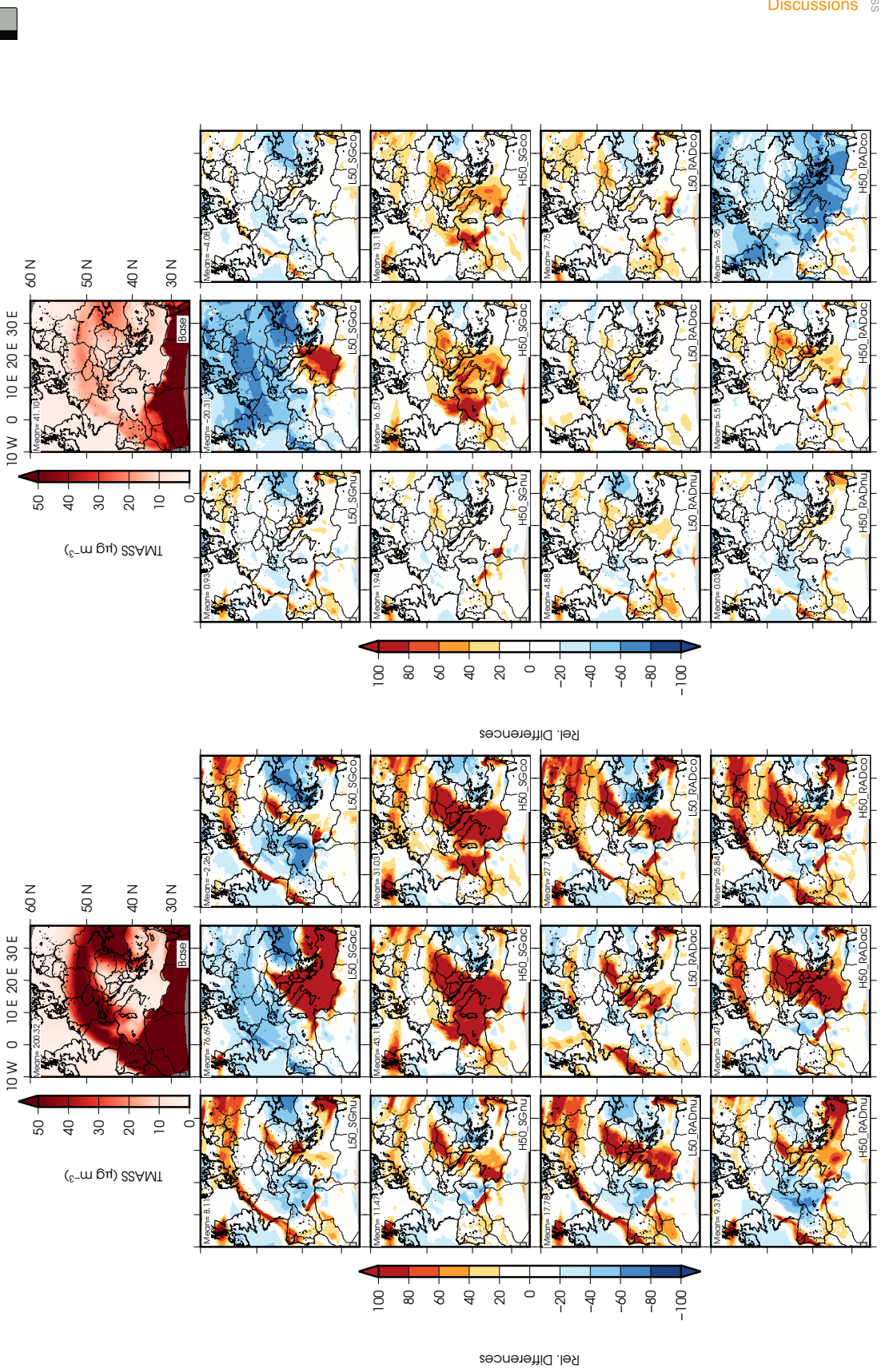


**Figure 5.** Id. 4 but for total mass concentration.

https://doi.org/10.5194/gmd-2020-68
Preprint. Discussion started: 28 April 2020


Geoscientific Model Development Discussions

### 3.4 Discussion: uncertainties in DG and SG regarding observations

A question arising from the results presented so far relies not only on which modification presents the highest sensitivity for modifying AOD, but also how the modifications implemented in the GOCART aerosol scheme (which assumes the fixed size distribution defined in Table 1 for each experiment) compare with observations. In this sense, this section tries to bring some light on the relationship between our findings and observed aerosol size distributions available in the scientific literature. To cope with that, Table 3 summarizes observed DG and SG found through a comprehensive review.

**Table 1.** DG and SG values in our experiments (DG in $\mu$m).

| | Aitken | | Accumulation | | Coarse | |
|---|---|---|---|---|---|---|
| | DG | SG | DG | SG | DG | SG |
| Base | 0.010 | 1.70 | 0.070 | 2.00 | 1.0 | 2.50 |
| L10 | 0.009 | 1.53 | 0.063 | 1.80 | 0.9 | 2.25 |
| H10 | 0.011 | 1.87 | 0.077 | 2.20 | 1.1 | 2.75 |
| L20 | 0.008 | 1.36 | 0.056 | 1.60 | 0.8 | 2.00 |
| H20 | 0.012 | 2.04 | 0.084 | 2.40 | 1.2 | 3.00 |
| L50 | 0.005 | 0.85 | 0.035 | 1.00 | 0.5 | 1.25 |
| H50 | 0.015 | 2.55 | 0.105 | 3.00 | 1.5 | 3.75 |

Table 3 is representative of the large uncertainty existing the characterizing the different modes of aerosol distribution. These values have been derived from a wide range of environments and over various locations worldwide. Regarding the geometric diameter, none of the works reviewed displays a three-mode size distribution analogous to the parameters used in GOCART (base case).

However, some similarities can be found. Regarding the smallest particles, the GOCART model represents an only mode (Aitken), whose values are similar to those modes called by Covert et al. (1996) ultrafine; or by Mäkelä et al. (2000) or Rissler et al. (2006) nucleation. Vakkari et al. (2013) found similar but higher values for a ultrafine/nucleation mode. Thus, our experiment in which DG increases (H10, H20 and H50_DGai) will represent better this mode. However, even the H50_DGai experiment displays lower values (0.015) than those found by Tunved et al. (2003) (0.0294 and 0.0308) in the boundary layer over the Scandinavian Peninsula. So GOCART model seems to be underestimating the DG for the Aitken mode over the target domain, and the H50_DGai could contribute to enhance the skills of the modeling results.

The so-called Aitken mode by Covert et al. (1996); Mäkelä et al. (2000); Tunved et al. (2003); Rissler et al. (2006) and Brock et al. (2011) shows similar value to the mode 2 in Porter and Clarke (1997); Vakkari et al. (2013) and Marinescu et al. (2019). These values are slightly smaller or in the range of the mode named in the GOCART model as accumulation. Again, the cases in which DG for the accumulation mode is increased will improve the representation of this mode. Moreover, the decrease in the DG for the accumulation mode is one of the cases with noticeable differences for AOD. Thus, special attention should be paid for a correct definition of this mode.

https://doi.org/10.5194/gmd-2020-68
Preprint. Discussion started: 28 April 2020


Geoscientific Model Development Discussions

Finally, our model considers a coarse mode with a DG of 1$\mu$m. Again, this value is underestimated because the literature reviewed (Table 3) found coarse mode DG with values higher than 2 (maximum value of 1.5 in our H50 experiment) and up to 30. Thus, particles in our model are modelled smaller than those observed. Moreover, the increase of the DG in the coarse mode is one of the case in which AOD shows noticeable differences. Marinescu et al. (2019) found a mode number 4 with DG lower but close to the coarse mode in out simulations. Henceforth, increasing the DG in the coarse mode in GOCART model could contribute to improve the results of AOD in our simulations.

Values taken by SG in our base case are similar to those reported by Whitby (1978). However, observed SG are highly uncertain. Most of these works found SG values lower than those used in our base case for all of the modes, ultrafine/nucleation, which correspond with our Aitken; Aitken and accumulation, which are represented by our accumulation and coarse modes. Tunved et al. (2003) observed SG values similar to the ones used for the Aitken mode in the base case (1.70), both in winter and summer in the boundary layer over the Scandinavian Peninsula. However, this value is underestimated in comparison with the measurement carried out by Rissler et al. (2006); Vakkari et al. (2013) and Marinescu et al. (2019).

Whitby et al. (1972) is the only work in which SG value is higher than 2 for the accumulation mode. The rest of works reported lower values than the value used by GOCART in the base case. Probably because of that, the reduction in this parameter is the case which shows a higher influence in AOD representation (for all the experiments 10, 20 and 50%). As also happened for the accumulation mode, the SG in the base case for the coarse mode is highly overpredicted by the model when comparing its value with observations available in the literature.

## 4 Summary and Conclusions

Among others, aerosol size distribution is a key property of atmospheric aerosols which largely determines their interaction with radiation and clouds. This occurs because optical properties (as AOD) are strongly dependent on aerosol size distribution. Moreover, this distribution holds a strong influence on ARI and the associated radiative forcing. Henceforth, the main objective of this work is to study the impact of the representation of aerosol size distribution on aerosol optical properties over central Europe, and particularly over the Mediterranean Basin during the summertime. The case study has been selected because the Mediterranean Basin presents an intense formation, accumulation and recirculation of aerosols from different sources intensified during this summer episode.

In order to fulfill the objectives, a sensitivity test has been carried out in which the parameters which define a log-normal size distribution have been modified by $\pm$10, 20 and 50 %.

The sensitivity test reveals that the modification (lowering) in the standard deviation of the accumulation mode (L_SGac) presents the highest sensitivity with respect to the AOD representation. This modification provokes a narrowed distribution in the accumulation mode which results in two different scenarios: (1) over those areas where fire particles predominate in the base case, particles transfer from the accumulation to the coarse mode resulting in an increase of the total number and mass in the latter mode and an increase in AOD; and (2) over those areas where coarse particles dominate, particles are transferred from the accumulation to the coarse mode but this favors the removal of particles, reducing the total number and mass and

https://doi.org/10.5194/gmd-2020-68
Preprint. Discussion started: 28 April 2020


Geoscientific Model Development Discussions

hence the levels of AOD. This removal of particles of the coarse mode during atmospheric transport was previously observed by Maring et al. (2003).

The reduction of the standard deviation of the accumulation mode is the only experiment in which all of the sensitivities tests run present important influences on AOD. Moreover, the response for all of the sensitivities is similar and increases as the modification becomes larger.

The rest of the sensitivity experiments only shows important differences for the modification of 50 % in the target parameters. The experiment in which the diameter of the coarse mode is increased (H50_DGco) is the experiment with a higher influence on AOD. For this experiment, a redistribution through the total size distribution occurs due to the increase in the coarse diameter, which produces a relocation of number and mass particles from the finer modes to the coarse. The other experiment with an important response to the sensitivity test is the case in which the diameter of the accumulation mode is decreased (L50_DGac). In this case, the reduction observed in AOD could be attributed to the reduction in the diameter assumed by the log-normal distribution in the accumulation mode. Hence, although mass and number concentrations are similar, the model is assuming that particles in the accumulation mode are smaller than in the base case and this results in a reduction of AOD.

The comparison of size distribution parameters (DG and SG) in our simulations and observations reveals that, generally, the base case underestimates the geometric diameter in all modes. This underestimation is even more noticeable for the coarse mode. Moreover, a mode is missed for the fine particles. While the model displays two modes (Aitken and accumulation) for particles lower than 1$\mu$m, observations indicate the presence of three modes (ultrafine/nucleation, Aitken and accumulation). The differences found in our experiments when DG is modified in the accumulation and coarse mode evince the need to carefully consider the definition in GOCART of the value of this parameter.

On the other hand, the modification in the standard deviation for the accumulation mode in our sensitivity experiments is one of the cases with a higher influence in AOD levels. This fact, together with the high uncertainty in the measurement of this parameter reported by observations, should be taken into account in order to improve the representation of size distribution in aerosol models, in particular, in those that used a fix size distribution as GOCART.

This contribution identifies those cases where AOD exhibits a larger sensitivity to the target parameters. However, further experiments are needed in order to improve the representation of size distribution in models by using observational data (information for DG and SG from in-situ and remote sensing observations). Although a more accurate fixed size distribution could be defined, the use of any fixed has some limitations since aerosol size likely varies spatially/temporally as well. The improvement in this representation will reduce the uncertainty associated to aerosol effects on climate, in particular to ARI.

*Code and data availability.* WRF-Chem code used to perform this work as well as data presented here are available at doi:10.5281/zenodo.3768076

https://doi.org/10.5194/gmd-2020-68
Preprint. Discussion started: 28 April 2020


Geoscientific Model Development Discussions

*Author contributions.* LP-P wrote the manuscript, with contributions from PJ-G. LP-P, PJ-G and JF design the experiments; LP-P conducted the numerical simulations and compiled all the experiments. LP-P did the analysis, with the support of JF , EP-S and PJ-G.

*Competing interests.* The authors declare no conflict of interest.

*Acknowledgements.* The authors acknowledge the ACEX-CGL2017-87921-R project, funded by the Spanish Ministry of the Economy and Competitiveness and the European Regional Development Fund (ERDF/FEDER). Laura Palacios-Peña thanks the FPU14/05505 scholarship from the Spanish Ministry of Education, Culture and Sports and to the ERASMUS+ program. Jerome D. Fast was supported by the Atmospheric System Research (ASR) program as part of the U.S. Department of Energy's Office of Biological and Environmental Research

https://doi.org/10.5194/gmd-2020-68
Preprint. Discussion started: 28 April 2020




## References

Ackerman, T. P. and Toon, O. B.: Absorption of visible radiation in atmosphere containing mixtures of absorbing and nonabsorbing particles, Applied Optics, 20, 3661 – 3668, doi: 10.1364/AO.20.003661, 1981.

Andreae, M. and Rosenfeld, D.: Aerosol–cloud–precipitation interactions. Part 1. The nature and sources of cloud-active aerosols, Earth-Science Reviews, 89, 13 – 41, doi: 10.1016/j.earscirev.2008.03.001, 2008.

Andreae, M. O. and Merlet, P.: Emission of trace gases and aerosols from biomass burning, Global Biogeochemical Cycles, 15, 955 – 966, doi: 10.1029/2000GB001382, 2001.

Andreae, T. W., Andreae, M. O., Ichoku, C., Maenhaut, W., Cafmeyer, J., Karnieli, A., and Orlovsky, L.: Light scattering by dust and anthropogenic aerosol at a remote site in the Negev desert, Israel, Journal of Geophysical Research: Atmospheres, 107, doi: 10.1029/2001JD900252, 2002.

Barnard, J. C., Fast, J. D., Paredes-Miranda, G., Arnott, W. P., and Laskin, A.: Technical note: evaluation of the WRF-Chem "aerosol chemical to aerosol optical properties" module using data from the MILAGRO campaign, Atmospheric Chemistry and Physics, 10, 7325 – 7340, doi: 10.5194/acp-10-7325-2010, 2010.

Bohren, C. F. and Huffman, D. R.: Absorption and Scattering of Light by Small Particles, John Wiley & Sons, Ltd, 530 pages, doi: 10.1002/9783527618156, 2007.

Boucher, O.: Atmospheric Aerosols: Properties and Climate Impacts, Springer Netherlands, xVII, 311 pages, doi: 10.1007/978-94-017-9649-1, 2015.

Boucher, O. and Anderson, T. L.: General circulation model assessment of the sensitivity of direct climate forcing by anthropogenic sulfate aerosols to aerosol size and chemistry, Journal of Geophysical Research: Atmospheres, 100, 26 117 – 26 134, doi: 10.1029/95JD02531, 1995.

Boucher, O., Schwartz, S. E., Ackerman, T. P., Anderson, T. L., Bergstrom, B., Bonnel, B., Chýlek, P., Dahlback, A., Fouquart, Y., Fu, Q., Halthore, R. N., Haywood, J. M., Iversen, T., Kato, S., Kinne, S., Kirkevåg, A., Knapp, K. R., Lacis, A., Laszlo, I., Mishchenko, M. I., Nemesure, S., Ramaswamy, V., Roberts, D. L., Russell, P., Schlesinger, M. E., Stephens, G. L., Wagener, R., Wang, M., Wong, J., and Yang, F.: Intercomparison of models representing direct shortwave radiative forcing by sulfate aerosols, Journal of Geophysical Research: Atmospheres, 103, 16 979 – 16 998, doi: 10.1029/98JD00997, 1998.

Boucher, O., Randall, D., Artaxo, P., Bretherton, C., Feingold, G., Forster, P., Kerminen, V.-M., Kondo, Y., Liao, H., Lohmann, U., Rasch, P., Satheesh, S., Sherwood, S., Stevens, B., and Zhang, X.: Clouds and aerosols, in: Climate Change 2013: The Physical Science Basis. Contribution of Working Group I to the Fifth Assessment Report of the Intergovernmental Panel on Climate Change, edited by Stocker, T., Qin, D., Plattner, G.-K., Tignor, M., Allen, S., Boschung, J., Nauels, A., Xia, Y., Bex, V., , and Midgley, P., pp. 571 – 657, Cambridge University Press, Cambridge University Press, Cambridge, United Kingdom and New York, NY, USA., 2013.

Brock, C. A., Cozic, J., Bahreini, R., Froyd, K. D., Middlebrook, A. M., McComiskey, A., Brioude, J., Cooper, O. R., Stohl, A., Aikin, K. C., de Gouw, J. A., Fahey, D. W., Ferrare, R. A., Gao, R.-S., Gore, W., Holloway, J. S., Hübler, G., Jefferson, A., Lack, D. A., Lance, S., Moore, R. H., Murphy, D. M., Nenes, A., Novelli, P. C., Nowak, J. B., Ogren, J. A., Peischl, J., Pierce, R. B., Pilewskie, P., Quinn, P. K., Ryerson, T. B., Schmidt, K. S., Schwarz, J. P., Sodemann, H., Spackman, J. R., Stark, H., Thomson, D. S., Thornberry, T., Veres, P., Watts, L. A., Warneke, C., and Wollny, A. G.: Characteristics, sources, and transport of aerosols measured in spring 2008 during the aerosol, radiation, and cloud processes affecting Arctic Climate (ARCPAC) Project, Atmospheric Chemistry and Physics, 11, 2423–2453, https://doi.org/10.5194/acp-11-2423-2011, 2011.

https://doi.org/10.5194/gmd-2020-68
Preprint. Discussion started: 28 April 2020




Brock, C. A., Wagner, N. L., Anderson, B. E., Beyersdorf, A., Campuzano-Jost, P., Day, D. A., Diskin, G. S., Gordon, T. D., Jimenez, J. L., Lack, D. A., Liao, J., Markovic, M. Z., Middlebrook, A. M., Perring, A. E., Richardson, M. S., Schwarz, J. P., Welti, A., Ziemba, L. D., and Murphy, D. M.: Aerosol optical properties in the southeastern United States in summer– Part 2: Sensitivity of aerosol optical depth to relative humidity and aerosol parameters, Atmospheric Chemistry and Physics, 16, 5009 – 5019, https://doi.org/10.5194/acp-16-5009-2016, 2016.

Buseck, P. and Schwartz, S.: 4.04 - Tropospheric Aerosols, in: Treatise on Geochemistry, edited by Holland, H. D. and Turekian, K. K., pp. 91 – 142, Pergamon, Oxford, doi: 10.1016/B0-08-043751-6/04178-5, 2003.

Charlson, R. J., Schwartz, S. E., Hales, J. M., Cess, R. D., Coakley, J. A., Hansen, J. E., and Hofmann, D. J.: Climate Forcing by Anthropogenic Aerosols, Science, 255, 423 – 430, doi: 10.1126/science.255.5043.423, 1992.

Chin, M., Ginoux, P., Kinne, S., Torres, O., Holben, B. N., Duncan, B. N., Martin, R. V., Logan, J. A., Higurashi, A., and Nakajima, T.: Tropospheric aerosol optical thickness from the GOCART model and comparisons with satellite and Sun photometer measurements, Journal of the Atmospheric Sciences, 59, 461 – 483, doi: 10.1175/1520-0469(2002)059<0461:TAOTFT>2.0.CO;2, 2002.

Claquin, T., Schulz, M., Balkanski, Y., and Boucher, O.: Uncertainties in assessing radiative forcing by mineral dust, Tellus B, 50, 491 – 505, doi: 10.1034/j.1600-0889.1998.t01-2-00007.x, 1998.

Covert, D. S., Wiedensohler, A., Aalto, P., Heintzenberg, J., Mcmurry, P. H., and Leck, C.: Aerosol number size distributions from 3 to 500 nm diameter in the arctic marine boundary layer during summer and autumn, Tellus B: Chemical and Physical Meteorology, 48, 197 – 212, https://doi.org/10.3402/tellusb.v48i2.15886, 1996.

Dee, D. P., Uppala, S. M., Simmons, A. J., Berrisford, P., Poli, P., Kobayashi, S., Andrae, U., Balmaseda, M. A., Balsamo, G., Bauer, P., Bechtold, P., Beljaars, A. C. M., van de Berg, L., Bidlot, J., Bormann, N., Delsol, C., Dragani, R., Fuentes, M., Geer, A. J., Haimberger, L., Healy, S. B., Hersbach, H., Hólm, E. V., Isaksen, L., Kållberg, P., Köhler, M., Matricardi, M., McNally, A. P., Monge-Sanz, B. M., Morcrette, J.-J., Park, B.-K., Peubey, C., de Rosnay, P., Tavolato, C., Thépaut, J.-N., and Vitart, F.: The ERA-Interim reanalysis: Configuration and performance of the data assimilation system, Quarterly Journal of the Royal Meteorological Society, 137, 553 – 597, doi: 10.1002/qj.828, 2011.

Deshler, T., Hervig, M. E., Hofmann, D. J., Rosen, J. M., and Liley, J. B.: Thirty years of in situ stratospheric aerosol size distribution measurements from Laramie, Wyoming (41°N), using balloon-borne instruments, Journal of Geophysical Research: Atmospheres, 108, https://doi.org/10.1029/2002JD002514, 2003.

Eck, T. F., Holben, B. N., Reid, J. S., Dubovik, O., Smirnov, A., O'Neill, N. T., Slutsker, I., and Kinne, S.: Wavelength dependence of the optical depth of biomass burning, urban, and desert dust aerosols, Journal of Geophysical Research: Atmospheres, 104, 31 333 – 31 349, doi: 10.1029/1999JD900923, 1999.

Geiger, H., Barnes, I., Bejan, I., Benter, T., and Spittler, M.: The tropospheric degradation of isoprene: an updated module for the regional atmospheric chemistry mechanism, Atmospheric Environment, 37, 1503 – 1519, doi: https://doi.org/10.1016/S1352-2310(02)01047-6, 2003.

Ginoux, P., Chin, M., Tegen, I., Prospero, J. M., Holben, B., Dubovik, O., and Lin, S.-J.: Sources and distributions of dust aerosols simulated with the GOCART model, Journal of Geophysical Research: Atmospheres, 106, 20 255 – 20 273, doi: 10.1029/2000JD000053, 2001.

Giorgi, F.: Climate change hot-spots, Geophysical Research Letters, 33, L08 707, doi: 10.1029/2006GL025734, 2006.

Grell, G. A. and Freitas, S. R.: A scale and aerosol aware stochastic convective parameterization for weather and air quality modeling, Atmospheric Chemistry and Physics, 14, 5233 – 5250, doi: 10.5194/acp-14-5233-2014, 2014.

https://doi.org/10.5194/gmd-2020-68
Preprint. Discussion started: 28 April 2020




Grell, G. A., Peckham, S. E., Schmitz, R., McKeen, S. A., Frost, G., Skamarock, W. C., and Eder, B.: Fully coupled "online" chemistry within the WRF model, Atmospheric Environment, 39, 6957 – 6975, doi: 10.1016/j.atmosenv.2005.04.027, 2005.

Guenther, A., Karl, T., Harley, P., Wiedinmyer, C., Palmer, P. I., and Geron, C.: Estimates of global terrestrial isoprene emissions using MEGAN (Model of Emissions of Gases and Aerosols from Nature), Atmospheric Chemistry and Physics, 6, 3181 – 3210, doi: 10.5194/acp-6-3181-2006, 2006.

Haywood, J. and Boucher, O.: Estimates of the direct and indirect radiative forcing due to tropospheric aerosols: A review, Reviews of Geophysics, 38, 513 – 543, doi: 10.1029/1999RG000078, 2000.

Hinds, W. C.: Aerosol technology: properties, behavior, and measurement of airborne particles, John Wiley & Sons, second edn., 504 pages, 2012.

Hong, S.-Y., Noh, Y., and Dudhia, J.: A New Vertical Diffusion Package with an Explicit Treatment of Entrainment Processes, Monthly Weather Review, 134, 2318 – 2341, doi: 10.1175/MWR3199.1, 2006.

Iacono, M. J., Delamere, J. S., Mlawer, E. J., Shephard, M. W., Clough, S. A., and Collins, W. D.: Radiative forcing by long-lived greenhouse gases: Calculations with the AER radiative transfer models, Journal of Geophysical Research: Atmospheres, 113, D13 103, doi: 10.1029/2008JD009944, 2008.

Janssens-Maenhout, G., Dentener, F., Van Aardenne, J., Monni, S., Pagliari, V., Orlandini, L., Klimont, Z., Kurokawa, J.-i., Akimoto, H., Ohara, T., et al.: EDGAR-HTAP: a harmonized gridded air pollution emission dataset based on national inventories, Tech. rep., European Commission Joint Research Centre Institute for Environment and Sustainability., Luxembourg, #JRC58434, pages 42, doi: 10.2788/14102, 2012.

Mäkelä, J. M., Koponen, I. K., Aalto, P., and Kulmala, M.: ONE-YEAR DATA OF SUBMICRON SIZE MODES OF TROPOSPHERIC BACKGROUND AEROSOL IN SOUTHERN FINLAND, Journal of Aerosol Science, 31, 595 – 611, https://doi.org/10.1016/S0021-8502(99)00545-5, 2000.

Marinescu, P. J., Levin, E. J. T., Collins, D., Kreidenweis, S. M., and van den Heever, S. C.: Quantifying aerosol size distributions and their temporal variability in the Southern Great Plains, USA, Atmospheric Chemistry and Physics, 19, 11 985 – 12 006, https://doi.org/10.5194/acp-19-11985-2019, 2019.

Maring, H., Savoie, D. L., Izaguirre, M. A., Custals, L., and Reid, J. S.: Mineral dust aerosol size distribution change during atmospheric transport, Journal of Geophysical Research: Atmospheres, 108, 8592, doi: 10.1029/2002JD002536, 2003.

Millán, M. M., Salvador, R., Mantilla, E., and Kallos, G.: Photooxidant dynamics in the Mediterranean basin in summer: results from European research projects, Journal of Geophysical Research: Atmospheres, 102, 8811 – 8823, doi: 10.1029/96JD03610, 1997.

Morrison, H., Thompson, G., and Tatarskii, V.: Impact of Cloud Microphysics on the Development of Trailing Stratiform Precipitation in a Simulated Squall Line: Comparison of One- and Two-Moment Schemes, Monthly Weather Review, 137, 991 – 1007, doi: 10.1175/2008MWR2556.1, 2009.

Myhre, G. and Stordal, F.: Global sensitivity experiments of the radiative forcing due to mineral aerosols, Journal of Geophysical Research: Atmospheres, 106, 18 193 – 18 204, doi: 10.1029/2000JD900536, 2001.

Obiso, V. and Jorba, O.: Aerosol-radiation interaction in atmospheric models: Idealized sensitivity study of simulated short-wave direct radiative effects to particle microphysical properties, Journal of Aerosol Science, 115, 46 – 61, doi: 10.1016/j.jaerosci.2017.10.004, 2018.

Obiso, V., Pandolfi, M., Ealo, M., and Jorba, O.: Impact of aerosol microphysical properties on mass scattering cross sections, Journal of Aerosol Science, 112, 68 – 82, doi: 10.1016/j.jaerosci.2017.03.001, 2017.

https://doi.org/10.5194/gmd-2020-68
Preprint. Discussion started: 28 April 2020




Palacios-Peña, L., Baró, R., Guerrero-Rascado, J. L., Alados-Arboledas, L., Brunner, D., and Jiménez-Guerrero, P.: Evaluating the representation of aerosol optical properties using an online coupled model over the Iberian Peninsula, Atmospheric Chemistry and Physics, 17, 277 – 296, doi: 10.5194/acp-17-277-2017, 2017.

Palacios-Peña, L., Baró, R., Baklanov, A., Balzarini, A., Brunner, D., Forkel, R., Hirtl, M., Honzak, L., López-Romero, J. M., Montávez, J. P., Pérez, J. L., Pirovano, G., San José, R., Schröder, W., Werhahn, J., Wolke, R., Žabkar, R., and Jiménez-Guerrero, P.: An assessment of aerosol optical properties from remote-sensing observations and regional chemistry–climate coupled models over Europe, Atmospheric Chemistry and Physics, 18, 5021 – 5043, doi: 10.5194/acp-18-5021-2018, 2018.

Palacios-Peña, L., Jiménez-Guerrero, P., Baró, R., Balzarini, A., Bianconi, R., Curci, G., Landi, T. C., Pirovano, G., Prank, M., Riccio, A., Tuccella, P., and Galmarini, S.: Aerosol optical properties over Europe: an evaluation of the AQMEII Phase 3 simulations against satellite observations, Atmospheric Chemistry and Physics, 19, 2965 – 2990, doi: 10.5194/acp-19-2965-2019, 2019a.

Palacios-Peña, L., Lorente-Plazas, R., Montávez, J. P., and Jiménez-Guerrero, P.: Saharan Dust Modeling Over the Mediterranean Basin and Central Europe: Does the Resolution Matter?, Frontiers in Earth Science, 7, 290, doi: 10.3389/feart.2019.00290, 2019b.

Papadimas, C. D., Hatzianastassiou, N., Matsoukas, C., Kanakidou, M., Mihalopoulos, N., and Vardavas, I.: The direct effect of aerosols on solar radiation over the broader Mediterranean basin, Atmospheric Chemistry and Physics, 12, 7165 – 7185, doi: 10.5194/acp-12-7165-2012, 2012.

Pérez, C., Sicard, M., Jorba, O., Comerón, A., and Baldasano, J. M.: Summertime re-circulations of air pollutants over the north-eastern Iberian coast observed from systematic EARLINET lidar measurements in Barcelona, Atmospheric Environment, 38, 3983 – 4000, doi: 10.1016/j.atmosenv.2004.04.010, 2004.

Petzold, A., Weinzierl, B., Huntrieser, H., Stohl, A., Real, E., Cozic, J., Fiebig, M., Hendricks, J., Lauer, A., Law, K., Roiger, A., Schlager, H., and Weingartner, E.: Perturbation of the European free troposphere aerosol by North American forest fire plumes during the ICARTT-ITOP experiment in summer 2004, Atmospheric Chemistry and Physics, 7, 5105 – 5127, https://doi.org/10.5194/acp-7-5105-2007, 2007.

Porter, J. N. and Clarke, A. D.: Aerosol size distribution models based on in situ measurements, Journal of Geophysical Research: Atmospheres, 102, 6035 – 6045, https://doi.org/10.1029/96JD03403, 1997.

Querol, X., Alastuey, A., Pey, J., Cusack, M., Pérez, N., Mihalopoulos, N., Theodosi, C., Gerasopoulos, E., Kubilay, N., and Koçak, M.: Variability in regional background aerosols within the Mediterranean, Atmospheric Chemistry and Physics, 9, 4575 – 4591, doi: 10.5194/acp-9-4575-2009, 2009.

Remer, L. A., Kaufman, Y. J., Holben, B. N., Thompson, A. M., and McNamara, D.: Biomass burning aerosol size distribution and modeled optical properties, Journal of Geophysical Research: Atmospheres, 103, 31 879 – 31 891, https://doi.org/10.1029/98JD00271, 1998.

Rissler, J., Vestin, A., Swietlicki, E., Fisch, G., Zhou, J., Artaxo, P., and Andreae, M. O.: Size distribution and hygroscopic properties of aerosol particles from dry-season biomass burning in Amazonia, Atmospheric Chemistry and Physics, 6, 471 – 491, https://doi.org/10.5194/acp-6-471-2006, 2006.

Romakkaniemi, S., Arola, A., Kokkola, H., Birmili, W., Tuch, T., Kerminen, V.-M., Räisänen, P., Smith, J. N., Korhonen, H., and Laaksonen, A.: Effect of aerosol size distribution changes on AOD, CCN and cloud droplet concentration: Case studies from Erfurt and Melpitz, Germany, Journal of Geophysical Research: Atmospheres, 117, D07 202, doi: 10.1029/2011JD017091, 2012.

Seinfeld, J. H. and Pandis, S. N.: Atmospheric Chemistry and Physics: From Air Pollution to Climate Change, John Wiley & Sons, INC., Second edn., 1225 pages, 2006.

Soares, J., Sofiev, M., and Hakkarainen, J.: Uncertainties of wild-land fires emission in AQMEII phase 2 case study, Atmospheric Environment, 115, 361 – 370, doi: 10.1016/j.atmosenv.2015.01.068, 2015.

https://doi.org/10.5194/gmd-2020-68
Preprint. Discussion started: 28 April 2020




Sofiev, M., Vankevich, R., Lotjonen, M., Prank, M., Petukhov, V., Ermakova, T., Koskinen, J., and Kukkonen, J.: An operational system for the assimilation of the satellite information on wild-land fires for the needs of air quality modelling and forecasting, Atmospheric Chemistry and Physics, 9, 6833 – 6847, doi: 10.5194/acp-9-6833-2009, 2009.

Stephens, M. A.: EDF Statistics for Goodness of Fit and Some Comparisons, Journal of the American Statistical Association, 69, 730 – 737, doi: 10.1080/01621459.1974.10480196, 1974.

Stockwell, W. R., Kirchner, F., Kuhn, M., and Seefeld, S.: A new mechanism for regional atmospheric chemistry modeling, Journal of Geophysical Research: Atmospheres, 102, 25 847 – 25 879, doi: 10.1029/97JD00849, 1997.

Tanré, D., Kaufman, Y. J., Holben, B. N., Chatenet, B., Karnieli, A., Lavenu, F., Blarel, L., Dubovik, O., Remer, L. A., and Smirnov, A.: Climatology of dust aerosol size distribution and optical properties derived from remotely sensed data in the solar spectrum, Journal of Geophysical Research: Atmospheres, 106, 18 205 – 18 217, https://doi.org/10.1029/2000JD900663, 2001.

Tegen, I. and Lacis, A. A.: Modeling of particle size distribution and its influence on the radiative properties of mineral dust aerosol, Journal of Geophysical Research: Atmospheres, 101, 19 237 – 19 244, doi: 10.1029/95JD03610, 1996.

Tewari, M., Chen, F., Wang, W., Dudhia, J., LeMone, M., Mitchell, K., Ek, M., Gayno, G., Wegiel, J., and Cuenca, R.: Implementation and verification of the unified NOAH land surface model in the WRF model, in: 20th conference on weather analysis and forecasting/16th conference on numerical weather prediction, pp. 11 – 15, 2004.

Tunved, P., Hansson, H.-C., Kulmala, M., Aalto, P., Viisanen, Y., Karlsson, H., Kristensson, A., Swietlicki, E., Dal Maso, M., Ström, J., and Komppula, M.: One year boundary layer aerosol size distribution data from five nordic background stations, Atmospheric Chemistry and Physics, 3, 2183 – 2205, https://doi.org/10.5194/acp-3-2183-2003, 2003.

Vakkari, V., Beukes, J. P., Laakso, H., Mabaso, D., Pienaar, J. J., Kulmala, M., and Laakso, L.: Long-term observations of aerosol size distributions in semi-clean and polluted savannah in South Africa, Atmospheric Chemistry and Physics, 13, 1751 – 1770, https://doi.org/10.5194/acp-13-1751-2013, 2013.

Wesely, M. L.: Parameterization of surface resistances to gaseous dry deposition in regional-scale numerical models, Atmospheric Environment (1967), 23, 1293 – 1304, doi: 10.1016/0004-6981(89)90153-4, 1989.

Whitby, K., Husar, R., and Liu, B.: The aerosol size distribution of Los Angeles smog, Journal of Colloid and Interface Science, 39, 177 – 204, https://doi.org/10.1016/0021-9797(72)90153-1, 1972.

Whitby, K. T.: The physical characteristics of sulfur aerosols, Atmospheric Environment (1967), 12, 135 – 159, https://doi.org/10.1016/0004-6981(78)90196-8, 1978.

Wiedinmyer, C., Akagi, S. K., Yokelson, R. J., Emmons, L. K., Al-Saadi, J. A., Orlando, J. J., and Soja, A. J.: The Fire INventory from NCAR (FINN): a high resolution global model to estimate the emissions from open burning, Geoscientific Model Development, 4, 625 – 641, doi: 10.5194/gmd-4-625-2011, 2011.

Wild, O., Zhu, X., and Prather, M. J.: Fast-J: Accurate Simulation of In- and Below-Cloud Photolysis in Tropospheric Chemical Models, Journal of Atmospheric Chemistry, 37, 245 – 282, https://doi.org/10.1023/A:1006415919030, 2000.

https://doi.org/10.5194/gmd-2020-68
Preprint. Discussion started: 28 April 2020


Geoscientific Model Development Discussions
Open Access
EGU

**Table 2.** Summary of published observed log-normal size distribution parameters.

| Reference | Location | Measurement range | Environment | Mode* | Range ($\mu$m) | DG ($\mu$m) | SG |
|---|---|---|---|---|---|---|---|
| Whitby et al. (1972) | Pasadena (CA,US) | 0.003–6.8 | smog aerosol | ac | $< 1$ | 0.302 | 2.25 |
| | | | | co | 1 -15 | 7–10 | NA |
| Whitby (1978) | – | Review | – | nu | NA | 0.015-0.04 | 1.6 |
| | | | | ac | NA | 0.15-0.5 | 1.6-2.2 |
| | | | | co | NA | 5-30 | 2-3 |
| Covert et al. (1996) | Artic Ocean | 0.003-0.5 | Marine BL[1] | ul* | NA | 0.014±0.00042 | 1.36±0.50 |
| | | | | ai | NA | 0.045±0.00033 | 1.50±0.44 |
| | | | | ac | NA | 0.171±0.00027 | 1.64±0.25 |
| † Porter and Clarke (1997) | Pacific and Indian | 0.02-7.5 | Marine BL and FT[2] | 1 | NA | 0.179 | 1.46 |
| | | | | 2 | NA | 0.0765 | 1.61 |
| Remer et al. (1998) | Amazon Basin | 0.10-8 | BB[3] plume | ac | NA | 0.13±0.02 | 0.60 ± 0.04 |
| | | | | co | 6-40 | 11.5 | 1.23±0.23 |
| Mäkelä et al. (2000) | Hyytiälä (Finland) | 0.003-0.5 | boreal forest | nu | NA | 0.01548 | 1.47 |
| | | | | ai | NA | 0.05228 | 1.53 |
| | | | | ac | NA | 0.2039 | 1.40 |
| • Tanré et al. (2001) | Banizoumbou[a] | 0.10-6.0 | Dust Aerosol | ac | NA | 0.23 | NA |
| | | | | co | 1-5 | 2.19 | NA |
| | Sal Island[b] | | | ac | NA | 0.20 | NA |
| | | | | co | 1-5 | 2.15 | NA |
| | Sede Boker[c] | | | ac | NA | 0.13 | NA |
| | | | | co | 1-5 | 3.01 | NA |
| Deshler et al. (2003) | Stratocpheric (20km) Wyoming USA | 0.15-2 | Volcanic | 1 | NA | 0.13 | 1.26 |
| | | | | 2 | NA | 0.41 | 1.30 |
| | | | Background | 1 | NA | 0.69 | 1.63 |
| | | | | 2 | NA | 0.42 | 1.11 |
| ‡ Tunved et al. (2003) | Scandinavian Peninsula | 0.003-0.9 | BL(Winter) | nu | <0.03 | 0.0294 | 1.72 |
| | | | | ai | 0.03-0.11 | 0.0643 | 1.65 |
| | | | | ac | 0.11-1 | 0.198 | 1.50 |
| | | | BL(Summer) | nu | <0.03 | 0.0308 | 1.63 |
| | | | | ai | 0.03-0.11 | 0.0649 | 1.55 |
| | | | | ac | 0.11-1 | 0.187 | 1.17 |
| Rissler et al. (2006) | Rondonia[d] | 0.003-3.3 | BB plumes | nu | NA | 0.012 | 2.00-2.13 |
| | | | | ai | NA | 0.061-0.092 | 1.50-1.74 |
| | | | | ac | NA | 0.128-0.190 | 1.48-1.55 |

to continue

https://doi.org/10.5194/gmd-2020-68
Preprint. Discussion started: 28 April 2020


Geoscientific Model Development Discussions

**Table 3.** Summary of published observed log-normal size distribution parameters (second part).

| Reference | Location | Measurement range | Environment | Mode* | Range ($\mu$m) | DG ($\mu$m) | SG |
|---|---|---|---|---|---|---|---|
| Petzold et al. (2007) | European west coast | 0.004-20 | Transported BB plume | ac | NA | 0.25-0.3 | 1.30 |
| Brock et al. (2011) | Denver, Florida, Alaska, and Artic | 0.004 - 8.3 | Sea-ice BL | ac | NA | 0.178 | 1.52 |
| | | | FT background haze | ai | NA | 0.008-0.05 | NA |
| | | | | ac | NA | 0.17 | 1.54 |
| | | | | co | 1 - 5 | NA | NA |
| | | | Anthropogenic plumes | ac | NA | 0.174 | 1.54 |
| | | | BB plumes | ac | NA | 0.189 | 1.50 |
| | | | | co | NA | ∼4 | NA |
| Vakkari et al. (2013) | Botsalano[e] | 0.012-0.84 | Anthropogenic plumes | 1 | NA | 0.0181 | 2.02 |
| | | | | 2 | NA | 0.0602 | 2.00 |
| | | | | 3 | NA | 0.185 | 1.39 |
| | Marikana[e] | | | 1 | NA | 0.0129 | 1.87 |
| | | | | 2 | NA | 0.0535 | 2.07 |
| | | | | 3 | NA | 0.2056 | 1.30 |
| Brock et al. (2016) | South-East US | 0.004-1.0 | summertime lower troposphere | NA | NA | 0.12-0.17 | 1.42-1.60 |
| Marinescu et al. (2019) | Southern Great Plains, USA | 0.007-14 | Rural, continental site | 1 | NA | 0.0053 | 2.80 |
| | | | | 2 | NA | 0.05866 | 1.82 |
| | | | | 3 | NA | 0.16624 | 1.53 |
| | | | | 4 | NA | 0.82355 | 1.97 |

†Mean of 9 cases; ●DG=effective radius; ‡Winter=Sep-Feb mean, Summer=Mar-Aug mean over different locations
[a]Niger; [b]Cape Verde; [c]Israel; [d]Amazon region; [e]South Africa
[1]BL=Boundary layer; [2]FT=Free troposphere; [3]BB=Biomass Burning
*nu=nucleation, ul=ultrafine